Marine and Coastal Fisheries: Dynamics, Management, and Ecosystem Science 14:e10223, 2022

ISSN: 1942-5120 online
DOI: 10.1002/mcf2.10223

ARTICLE

Life History Assessment of Cusk, a Data-Poor Species, in U.S. Waters

W. David McElroy*
National Oceanic and Atmospheric Administration Fisheries, Northeast Fisheries Science Center, 166 Water Street, Woods Hole, Massachusetts 02543, USA

Emilee K. Tholke
IBSS Corporation, 1110 Bonifant Street, Suite 501, Silver Spring, Maryland 20910, USA; and Under contract to National Oceanic and Atmospheric Administration Fisheries, Northeast Fisheries Science Center, 166 Water Street, Woods Hole, Massachusetts 02543, USA

Mark J. Wuenschel and Eric Robillard
National Oceanic and Atmospheric Administration Fisheries, Northeast Fisheries Science Center, 166 Water Street, Woods Hole, Massachusetts 02543, USA

Abstract

Cusk *Brosme brosme* are fished across the northern Atlantic Ocean, but even basic biological data are limited in part by their difficult-to-sample deep and structured habitats. We sampled fish from a variety of sources across the Gulf of Maine to provide comprehensive life history information (age and size at maturity, fecundity, sex ratio, growth) for this data-poor species considered by National Oceanic and Atmospheric Administration Fisheries as a species of concern. Gonad histology and gonadosomatic index data indicated peak spawning in late spring (May–June), with limited spawning activity into summer. The histologically derived length at 50% maturity for female Cusk was 39.5 cm TL. Fecundity varied from a quarter million to four million oocytes, with a positive allometry versus size indicating that larger females have proportionally higher fecundity than smaller females. Male Cusk had unusually low gonadal investment for a gadiform, and males of all sizes examined (down to 21 cm) had spermatozoa present. Male maturity was equivocal even when the relative proportions of sperm stages were quantified through image analysis of gonad histology; further anatomical and physiological studies of small males are required to assess functional maturity in male cusk. The sex ratio at length indicated more males at larger sizes, and males had faster growth and larger size at age than females. Condition patterns also suggested lower condition for females than males after spawning and generally less variable condition for males. Gonadal investment, relative condition, and growth patterns all suggest differences in energy allocation between the sexes. This data-poor species has an uncertain stock status in U.S. waters; therefore, the results of the current work provide important information to its management.

The monospecific Cusk *Brosme brosme* occurs throughout the North Atlantic Ocean (from the Northeast U.S. Shelf to the European Shelf; Knutsen et al. 2009). They are found in deep, cold waters and are usually associated with rocky substrates in the Gulf of Maine (Auster and Lindholm 2005; Rountree and Juanes 2010), feeding on crustaceans, shellfish, and benthic fishes (Cohen et al. 1990). In the United States, commercial landings have

*Corresponding author: dave.mcelroy@noaa.gov
Received January 26, 2022; accepted August 16, 2022

declined from 500 to 2,400 metric tons per year from the 1960s to 1990s to less than 100 metric tons since 2004 (Hare et al. 2012). Although much of the decline in landings was due to changes in fishing activities, there is concern about the species due to their life history, preference for cold water, and recent warming in the region (Hare et al. 2012). In Canada, Cusk was listed as threatened in 2003 and endangered since 2012 (COSEWIC 2012), and the biomass index reference point is currently above the limit reference point but with a high uncertainty around it (DFO 2019). In the United States, a status review of Cusk was initiated in 2007, and it is still considered a candidate species under the Endangered Species Act by the National Oceanic and Atmospheric Administration (NOAA) (https://www.fisheries.noaa.gov/species/cusk). Unfortunately, due to their preferred (complex structured) habitats, Cusk are poorly sampled by bottom trawl surveys (e.g., Northeast Fisheries Science Center annual spring and autumn bottom trawl surveys; Hare et al. 2012; Tallack 2012; Ross et al. 2015), limiting the usefulness of bottom trawl time series to evaluate population trends (COSEWIC 2012). Limited sampling of rocky habitats preferred by Cusk has contributed to the hyperdepletion hypothesis for Cusk, where the trawl survey index declines faster than the population (Davies and Jonsen 2011; COSEWIC 2012). As a result, the status of the Canadian stock is assessed using the halibut longline survey index (DFO 2019). Perhaps related to their preferred deep and highly structured habitats and resulting scarcity in routine trawl surveys, many aspects of their life history in the northwest Atlantic Ocean are poorly understood and the stock is considered data poor.

In the northeast Atlantic Ocean, where *Brosme brosme* is referred to as tusk or törsk, a few studies report various aspects of life history, including age and growth (Bergstad and Hareide 1996; Bergstad et al. 1998; Jennings et al. 1999) and size at maturity (Bergstad and Hareide 1996; Magnússon et al. 1997; Magnussen 2007). Limited information exists on the reproductive biology of Cusk in the western Atlantic Ocean, largely limited to the work by Oldham (1972) on the Scotian Shelf. Several aspects of reproductive biology of Cusk (Oldham 1972) are similar to other gadids: having group-synchronous oocyte development, batch spawning, and determinate fecundity (Murua and Saborido-Rey 2003). However, Cusk tend to mature at larger sizes and older ages compared with Atlantic Cod *Gadus morhua*, Haddock *Melanogrammus aeglefinus*, and Pollock *Pollachius virens* (Magnussen 2007). Cohen et al. (1990) indicates spawning occurs April to July on both sides of the Atlantic Ocean. In the western Atlantic Ocean, spawning was reported to occur from March to November, inferred from eggs collected in ichthyoplankton surveys (Fahay 2007). Although movement and migration data are lacking, Cusk are not believed to form spawning aggregations (Oldham 1972; Knutsen et al. 2009). A study of genetic population structure throughout the North Atlantic Ocean indicated significant heterogeneity over short distances in some cases, supporting the idea of limited adult migration (Knutsen et al. 2009). In light of the demonstrated population heterogeneity for the species, detailed regional understanding of Cusk life history will help our limited understanding of Cusk biology and better inform the status evaluations and management.

The objectives of this study were to provide detailed information on Cusk life history in the northwest Atlantic Ocean (primarily in U.S. waters). Specifically, we sampled intensively with multiple fishing gear types to obtain large numbers and a wide range in size of Cusk to evaluate spawning seasonality, maturity, fecundity, sex ratio, condition, and age and growth. This study will help address the limited biological data for this species, which can help inform assessments of stock status and management in the USA and elsewhere.

METHODS

Sample collection.— Cusk samples (Table 1) were collected primarily during the spring (April–May) and fall (October–November) operations of the Northeast Fisheries Science Center (NEFSC) Gulf of Maine Bottom Longline Survey (BLLS; McElroy et al. 2019) and the NEFSC Bottom Trawl Survey (BTS; Politis et al. 2014). Additional samples in months outside the survey periods were obtained from commercial vessels participating in the NEFSC Study Fleet (Jones et al. 2022). These samples came from vessels using both bottom trawl and rod-and-reel gear. The BLLS covers only a portion of the Cusk range in the Gulf of Maine, but the BTS covers the entire gulf, including portions in Canadian waters and south to the continental shelf slope (Figure 1). The catch locations for the limited number of samples obtained from commercial fishers were not included on the map to protect the privacy of their fishing locations but were mostly located on the ledges of the central Gulf of Maine, with a few along the northern edge of Georges Bank.

Fish total length (TL; ±0.5 or ±0.1 cm), total body mass (TM; ±0.01 kg), gonad mass (GM; ±0.005 kg), and liver mass (LM; ±0.005 kg) were measured while at sea. An approximately 1-cm^3 piece of tissue was excised from the middle of one gonad and fixed in 10% neutral-buffered formalin.

The gonadosomatic index (GSI) and hepatosomatic index (HSI) were calculated as 100·{(gonad or liver) mass / [TM – (gonad or liver) mass]}, respectively (Wootton 1990). The length–mass relationship was determined for all points using a log-transformed linear model, $\ln(TM) = b \cdot \ln(TL) + \ln(a)$, where TM is total mass in kilograms, TL is total length in centimeters, and a and b are coefficients determined by least-squares regression. The model was fit

TABLE 1. Cusk samples ($n = 3{,}188$) summarized by sex, month, and each source: Northeast Fishery Science Center (NEFSC) Gulf of Maine Bottom Longline Survey (BLLS), NEFSC Bottom Trawl Survey (BTS), and the NEFSC Study Fleet (SF) program of collaborating commercial fishing vessels. Sample sizes for specific analyses may be smaller depending on the sample detail and quality.

Source	Years	Sex	n	Length range (cm)
BLLS	2014–2018	Female	1,439	26.0–92.7
	2014–2018	Male	1,527	27.9–91.0
	2014–2018	Unknown	6	42.9–80.6
BTS	2013–2018	Female	81	11.0–75.0
	2013–2018	Male	75	15.0–85.0
	2013–2018	Unknown	10	12.0–49.0
SF	2013–2017	Female	26	35.0–77.0
	2013–2017	Male	24	33.0–79.0

using least-squares regression in R software (version 3.5.3; www.r-project.org). The importance of sex as a factor in the length–mass model was evaluated using the aictab function from the AICcmodavg package, and the best model was selected using second-order Akaike information criterion (AIC_c) (Anderson 2008). Relative condition (K_n) was calculated as the ratio of the observed gonad-free mass over the predicted gonad-free body mass (Le Cren 1951) using a gonad-free length–mass equation for each sex to examine seasonal patterns.

Gonad histology.— The fixed ovarian and testes tissues were cut to <4 mm thickness, transferred to a histology cassette, and returned to formalin. The tissue samples were then dehydrated in a series of increasing ethyl alcohol concentrations and prepared using standard paraffin embedding techniques. The tissue was sectioned using a rotary microtome (5 µm), mounted on microscope slides, and stained with Schiffs–Mallory trichrome. Histology slides were projected onto a monitor using a microscope and camera for viewing and image capture (4–40×).

Female histology slides were assessed for the most advanced oocyte stage (MAOS), the presence and stage (early or late) of postovulatory follicles (POFs), occurrence and stage of atresia (alpha and beta), and tunica albuginea characteristics (Figure 2). The MAOS stages recorded were primary growth, cortical alveoli, early vitellogenesis, late vitellogenesis, germinal vesicle migration, hydrated, and ovulated. Primary growth oocytes have nucleoli visible around the periphery of the nucleus and no cytoplasmic inclusions. Cytoplasmic inclusions are seen in the cortical alveolar stage, appearing first as open circles and then later containing a dark staining inclusion. Early vitellogenic oocytes have yolk granules that appear around the periphery and advance inward until about halfway from the nucleus. Once yolk granules are beyond halfway and fill the entire cytoplasm surrounding the nucleus, the oocytes are considered in late vitellogenesis. Germinal vesicle migration (nucleus migration) begins as the nucleus migrates towards the edge of the oocyte where it will begin to breakdown. As the nucleus breaks down, the yolk granules fuse, the oocytes becomes hydrated, and the diameter increases but the oocytes

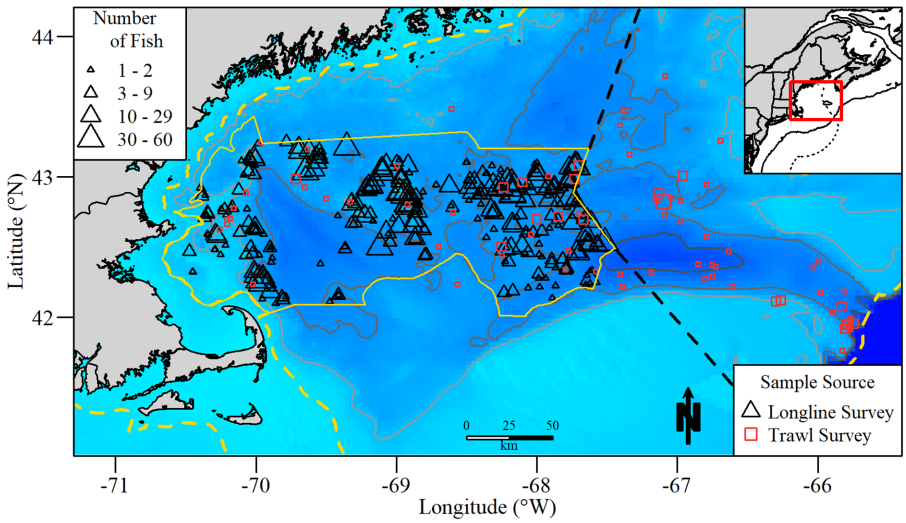

FIGURE 1. Distribution for Cusk sampled from the bottom trawl ($n = 166$) and bottom longline surveys ($n = 2{,}972$) in the Gulf of Maine. The solid yellow line indicates the outer boundary for the region covered by the bottom longline survey, and the dashed yellow line indicates the outer boundary of the offshore strata covered by the bottom trawl survey. The dashed black line indicates the United States exclusive economic zone maritime boundary. Bathymetric lines (gray) indicate increasing depth in 100-m intervals, with the darkest gray indicating 300 m. Points are scaled to the number of fish sampled at each location for samples from both surveys. Inset map includes the 300-m bathymetric contour (solid black).

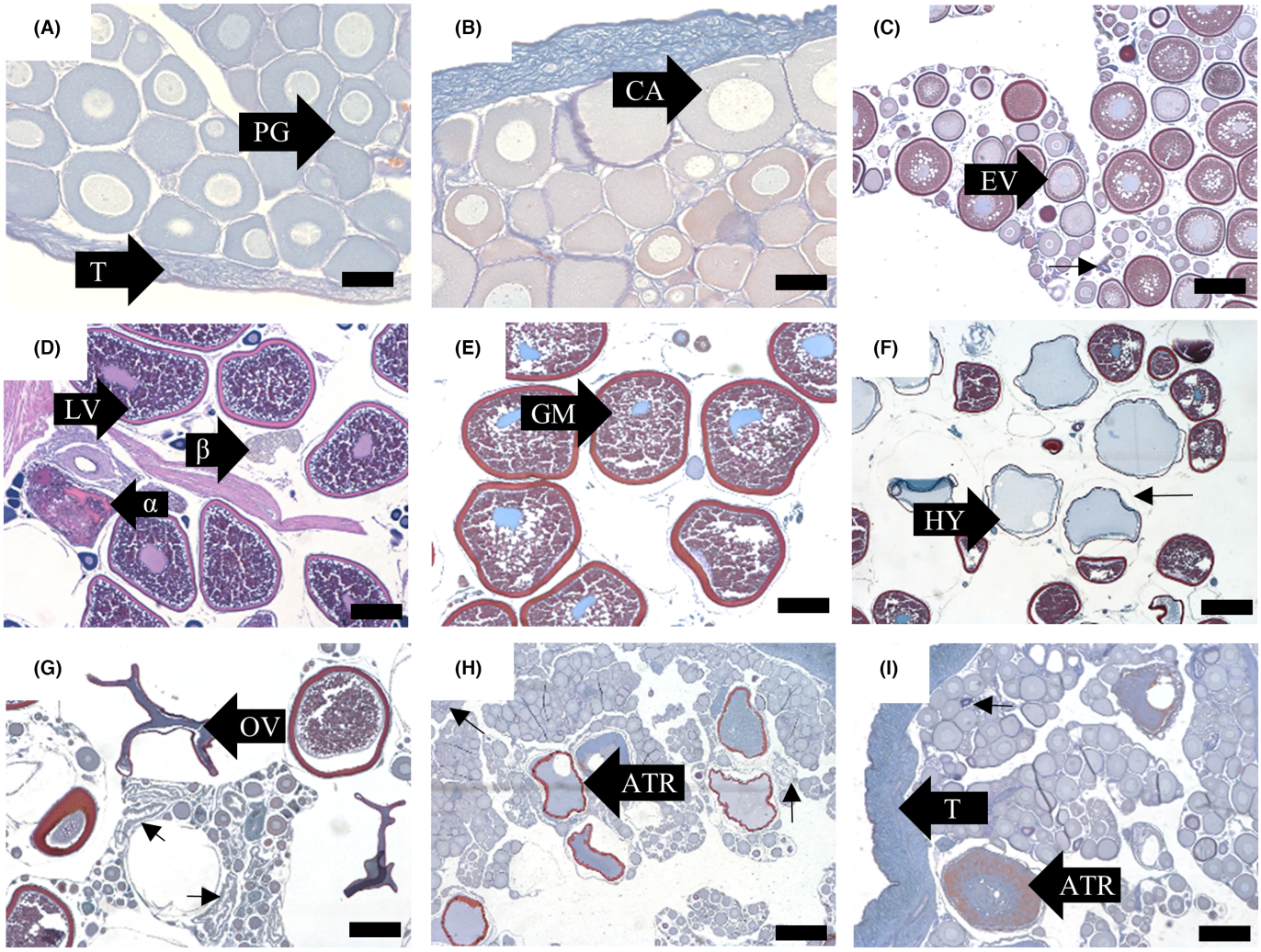

FIGURE 2. Transverse sections of Cusk ovaries with scale bars indicating **(A–B)** 50 μm, **(C–E), (G), (I)** 250 μm, and **(F), (H)** 500 μm. Panel (A) shows a sample from an immature female collected in April (38 cm TL) with primary growth oocytes (PG) and a simple tunica albuginea (T), and panel (B) shows an immature female sampled in November (43 cm TL) with a few cortical alveoli (CA) cells. The next panels show developing females sampled (C) in November (59 cm TL) with early vitellogenic oocytes (EV) and late postovulatory follicles (POFs; small arrow), (D) in May with late vitellogenic oocytes (LV; 56 cm TL) and alpha (α) and beta (β) atresia, and (E) in May (55 cm TL) with oocytes in germinal vesicle migration (GM). The following panels show (F) a ripe female (55 cm TL) captured in May with hydrated oocytes (HY) still within the follicle (small arrow), (G) a running ripe female captured in May (61 cm TL) with ovulated (OV) eggs released from the follicle and early POFs (small arrows), (H) a spent female (43 cm TL) sampled in November with PG oocytes, many atretic secondary growth cells (ATR), and POFs (small arrows), and (I) a resting female (45 cm TL) sampled in November with mostly PG oocytes, late POFs (small arrow), and ATR along with a complex tunica albuginea (T).

remain inside the follicle. Ovulation occurs once the fully hydrated oocytes are released from the follicle into the lumen of the ovary.

The POFs were classified into two stages, early and late (Figure 2), and were used as a spawning indicator. Early POFs had a double-layered string-like structure loosely arranged with a lumen (larger than primary growth oocytes). Late-stage POFs still appeared double layered but were more compact and much smaller than primary growth oocytes. Atretic cells were characterized as either alpha atresia, identified by the collapse and breakdown of the zona pellucida and yolk granules, or beta atresia, which had no yolk remaining and were reduced in size (smaller than primary growth oocytes; Figure 2). Tunica albuginea contains connective tissue and smooth muscle (McMillan 2007), and it was classified as either simple or complex. Simple tunica was thin with few layers of smooth muscle in cross section, while complex tunica was thicker, with multiple layers of smooth muscle present (Tholke et al. 2019).

Female maturity classes were defined similarly in both seasons, as POFs and hydrated oocytes were evident in both spring and fall (Table 2). For immature fish, the MAOS was usually primary growth or sometimes the early portion of the cortical alveoli stage (14 of 67 immature fish); all but 2 of these were in October and November. Oocyte development is protracted, with cortical alveoli appearing in summer soon after spawning and moving into early vitellogenesis for most mature fish by fall; therefore, we did not consider the presence of cortical alveoli as an indicator of maturity for the calendar year of collection. The complexity of the tunica was the key criteria distinguishing immature from resting classes, and the absence of POFs provided additional confirmation. The complex tunica of fish that had spawned previously was thicker with multiple layers of smooth muscle present. The resting class was the most similar to the immature fish, with an MAOS of cortical alveoli or occasionally primary growth (9% of resting fish) and the complex tunica distinguishing them from immature fish.

The early stages of vitellogenesis of the next year's cohort first appeared in the fall; therefore, the developing stage was divided into two classes. Early developing were defined by an MAOS of early vitellogenesis, and late developing had an MAOS of late vitellogenesis, with some fish showing signs of starting germinal vesicle migration (particularly in spring). The spent female class was distinguished from other classes using the MAOS (primary growth or cortical alveolar), POF presence, and the scale of atresia of remaining advanced oocytes (>50% of remaining secondary growth oocytes in alpha atresia). The ripe and running ripe classes were defined by the presence of hydrated and ovulated oocytes, respectively. Maturity was evaluated with samples from all seasons due to the presence of spawning activity and spawning markers from spring into late fall. Female maturity classification was considered relative to the calendar year of collection, which corresponded to ages assigned with a January 1 birthdate. A generalized linear model with a logit-link function was fit to binary (immature/mature) maturity data and TL.

Male histology slides were assessed for the most advanced spermatogenic stage, the dominant spermatogenic stage, and tunica development (Figure 3). Additional characters noted included the interstitial tissue (connective tissue seen throughout the teste section) and lumen (open space within the interstitial tissue). Four spermatogenic stages were identified. Spermatogonia were characterized by a large spherical germ cell with light granular cytoplasm and a spherical nucleus. Spermatocytes still had spherical cells but were smaller than spermatogonia. They divide to form spermatids. Spermatids were also characterized by a spherical cell but were smaller than spermatocytes. Spermatids do not divide but transform into spermatozoa. Spermatozoa become mobile due to the development of a flagellum. The dominant spermatogenic stage was the stage that composed >50% of cells in the section, even if spermatozoa was the most advanced stage present.

Macroscopic evaluation of Cusk revealed small testes that varied little in size seasonally, as indicated by the GSI. Microscopic evaluation of testes revealed advanced

TABLE 2. Histological characteristics used to define female maturity classes.

Maturity class	Characteristics
Immature	Most advanced oocyte stage is either primary growth (PG) or cortical alveolar (CA). Ovary compact with limited space between cells, no postovulatory follicles, and simple tunica albuginea without multiple layers of smooth muscle.
Early developing	Most advanced oocyte stage is early vitellogenic. May have older postovulatory follicles remaining from spawning in previous season.
Late developing	Ovaries with late vitellogenic oocytes as the most advanced stage. Final oocyte maturation may be just beginning, indicated by germinal vesicle migration. Some postovulatory follicles and/or atretic cells may be present. The tunica may be simple or complex.
Ripe	Hydrated or germinal vesicle breakdown oocytes present. Postovulatory follicles may be present.
Running ripe	Hydrated oocytes present outside the follicle (ovulated).
Spent (regressing)	Most advanced oocyte stage of PG or CA. Stages that are more advanced present but are resorbing with a majority of viable oocytes in PG and CA stages. A majority (>50%) or all of the advanced oocytes are atretic. Postovulatory follicles present.
Resting (regenerating)	Most advanced stage of PG or CA with any or all of the following: a complex tunica that has multiple smooth muscle layers, older postovulatory follicles, atretic of vitellogenic oocytes may be present.

sperm stages (i.e., spermatozoa) in small gonads of the smallest-size fish evaluated. Therefore, to better evaluate the functional maturity of males, we determined the spermatogenic maturity index (SMI, $n = 90$), which describes the area fraction of various cell stages, following Tomkiewicz et al. (2011). Nonoverlapping images (four to seven images per fish) from histological sections were evaluated using a point grid (24 points) overlaid on each image using the Grid function in ImageJ software (version 1.52d; National Institute of Health) with the Analyze and ObjectJ (version 1.04; University of Amsterdam) plugins. This included all ($n = 19$) small males (<40 cm TL) collected in the spring (April–June) with a sufficient slide quality and a subset of males ≥40 cm TL ($n = 71$; range = 41–87 cm TL). The spermatogenic cell stage, interstitial tissue, lumen, tunica, and any open space (due to tissue mounting) were recorded at each point on the grid (a cross was used as the grid point symbol; the tissue type that was present in the upper right quadrant was recorded). The area fraction of each cell type was calculated as the number of grid points for each cell type divided by the total number of points for testis tissue (Tomkiewicz et al. 2011). The tunica, lumen, and open space were excluded. The area fraction of each cell stage is then multiplied by a weighting factor to quantify the progression of spermatogenesis. The weighting factors used were interstitial tissue = 0, spermatogonia = 0.25, spermatocyte = 0.5, spermatids = 0.75, and spermatozoa = 1.0. The resulting SMI can range from 0 (only interstitial tissue present) to 1 (only spermatozoa).

Fecundity.— Fecundity was estimated for prespawn females with a MAOS in late vitellogenesis or germinal vesicle migration (2014: $n = 43$; 2015: $n = 52$; 2016: $n = 47$). Females were excluded if there were signs of spawning activity (germinal vesicle breakdown, hydrated oocytes, or postovulatory follicles). Gravimetric measurements of oocyte density (NG = number of oocytes per gram of ovary) were made from subsamples of fixed ovarian tissue that were patted dry and weighed (±0.0001 g), and a subsample size of 300–600 oocytes was targeted (~0.05–0.10 g). Subsamples were manipulated to separate the individual oocytes into a single layer, and images were taken with transmitted light using a dissecting scope and digital camera at 1.5×. ImageJ software with the ObjectJ plugin was used for image processing. Processing of images was made consistent between samples by use of a macro in ObjectJ modified from one developed for Atlantic Mackerel *Scomber scombrus* (A. Thorsen, Institute of Marine Research, personal communication). The macro automatically filtered the images and measured the oocyte diameters. Subsequent inspection of the processed image allowed correction of erroneously identified and measured particles (e.g., connective tissue or oocytes adhering to each other but not identified as separate objects). To avoid potential size bias, the diameters of oocytes damaged during sample processing were not included in the estimation of the mean, but the number of damaged cells was included in the total oocyte count for the subsample density (NG) in gravimetric subsamples.

The autodiametric relationship, oocyte density as a function of the mean oocyte diameter (OD), was modeled with a power function fit by least-squares regression. The autodiametric relationship was determined and reported to facilitate future fecundity estimates for the species. We modeled potential annual fecundity (PAF) as a function of fish length (TL) by the following: $\ln(\text{PAF}) = \beta_1 \cdot \ln(\text{TL}) + \alpha$, where α and β_1 are coefficients determined by least-squares fit regression. Fish TL was used as the measure of fish size as the total mass of fish is dynamic leading up to spawning. A base model with just TL was tested against a model including mean oocyte diameter of the leading cohort (OD_{LC}): $\ln(\text{PAF}) = \beta_1 \bullet \ln(\text{TL}) + \beta_2 \bullet (\text{OD}_{\text{LC}}) + \alpha$, where α, β_1, and β_2 are coefficients determined by least-squares fit regression. The OD_{LC} serves as an indicator for the individual time until spawning and therefore should account for some of the down-regulation that occurs in the lead up to spawning. The coefficient of slope for length of the final regression was tested against an isometric slope ($\beta_1 = b$, where b is the slope determined for the length-mass relationship) using a Wald test.

Age and growth.— Cusk sagittal otoliths were collected from the reproductively sampled fish as well as additional fish in 2016 and 2017 for age determination ($n = 1{,}041$). Otoliths were baked in an oven at 400°C for 1 min. They were read whole with a Leica M60 stereomicroscope using transmitted light at a magnification between 8× and 20×. A subsample of 52 samples were reread blindly to estimate percent agreement, coefficient of variation, (Campana and Jones 1992), and bias (Bowker 1948). The observed length-at-age data were fitted to the von Bertalanffy model (Ricker 1975). Likelihood ratio test (Kimura 1980) was used to determine if differences existed between growth parameter estimates between sexes for mean length-at-age data.

RESULTS

Size Distribution and Sex Ratio

The size distribution of the BLLS fish ranged from 26 to 93 cm but with most (97%) of the fish between 35 and 80 cm (Figure 4). The BTS samples were fewer in number, but they covered a broader length range (11–85 cm). The BTS accounted for most of the fish <30 cm (21 of 26 fish), and the BLLS accounted for most of the fish ≥80 cm (50 of 51 fish). The samples from the Cooperative Research Branch Study Fleet were intermediate in length (36–79 cm).

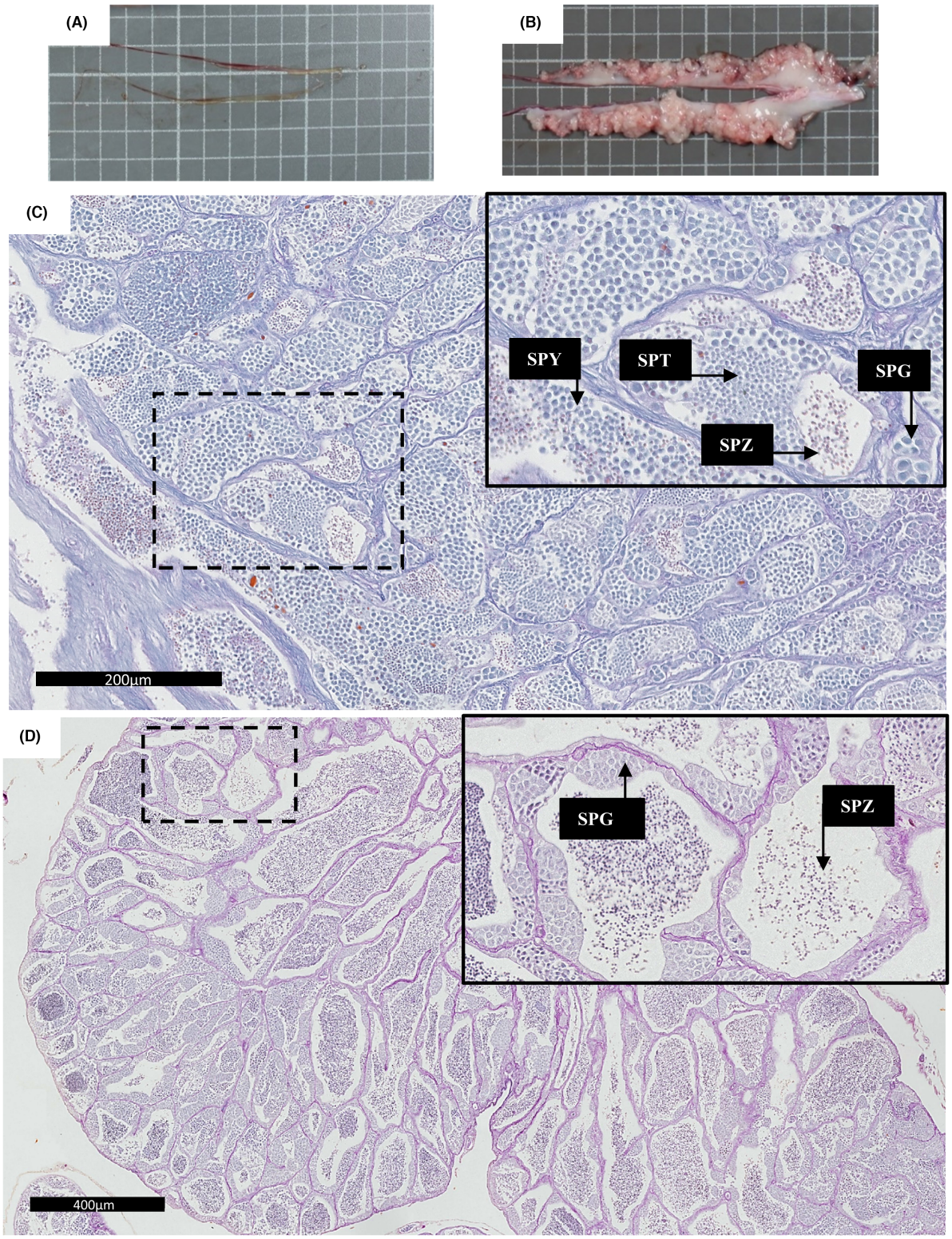

FIGURE 3. **(A–B)** Macroscopic images of whole testes and **(C–D)** transverse microscopic sections of a presumed immature and mature Cusk testes. Scale bars indicate (A–B) 2 cm, (C) 200 µm, and (D) 400 µm. Panels (A) and (C) show a presumed immature male (37 cm TL) collected in November with advanced sperm stages present, and panels (B) and (D) show a mature male (68.1 cm TL) collected in November with numerous lobules of spermatozoa. The spermatogenic stages labeled are spermatogonia (SPG), spermatocytes (SPY), spermatids (SPT), and spermatozoa (SPZ). Dashed boxes indicate the location of the inset image.

The length distributions by sex differed, with females peaking from 45 to 60 cm and male length numbers peaking from 60 to 80 cm (Figure 4). The mean length for females was 53.4 cm (SD = 9.5; $n = 1{,}634$) and was 5.6 cm below that of the male mean length of 59.0 cm (SD = 11.9; $n = 1{,}538$), which was significant (Student's $t = -14.6$, df = 2,933.7, $P < 0.01$). The sex ratio was skewed towards females (66–76%) between 42 and 56 cm (using 2-cm bins). The sex ratio was variable around 50% below 40 cm, although sample sizes were more limited (Figure 4). The ratio skewed towards males (>65%) starting at 62 cm and stayed above this, although the ratio fluctuated above 74 cm as sample sizes became smaller. Females were observed up to the largest sizes sampled.

Length–Mass Relationship

The length–mass relationship (Figure 5) for all sampled Cusk was $\ln(TM) = -12.1731 + 3.1695 \cdot \ln(TL)$, where TM is total fish mass in kilograms and TL is fish length in centimeters ($n = 3{,}160$; SE $a = 0.0333$, SE $b = 0.0083$; $r^2 = 0.98$). A length model including sex as a factor (only those fish with sex recorded: $n = 3{,}144$) was not an improvement over a model without sex ($\Delta AIC_c = 2.0$; without sex model weight = 0.73).

Female Reproductive Seasonality

The majority of samples were obtained from fishery independent surveys and concentrated in the spring and fall, with fewer fish sampled outside those months (Figure 6). Female spawning activity (ripe and running ripe fish) was observed starting in the middle of April (April 18 was the earliest spawning-active female sampled). Sample sizes in certain months limit the ability to precisely define the earliest or peak spawning activity, but based on the GSI, MAOS, and POFs, peak spawning was in late May and June. The majority of females in the spring were late developing. Spawning activity continued well into summer and even into fall. A few ripe females were observed in October and November (latest spawning-active fish was November 8), but most females were in a postspawning condition (spent or resting) or beginning the development of the next year's clutch in the fall (early developing). Early vitellogenesis was the most prevalent MAOS in the fall (Figure 6). The GSI was highest in April through June, but some females with higher GSI (>5) persisted into the fall months and, along with the MAOS, indicated protracted spawning by some individuals. The majority of females in the fall have a GSI < 3.

Spawning markers were present in females through the summer and fall, aiding the identification of mature spawning participants even after peak spawning season. Postovulatory follicle presence increased progressively into summer and persisted into the fall; POFs were present in 41.6% of mature females from October samples and 35.8% of November samples. Atresia (alpha and beta) was also present in most mature females (94.5%) sampled in October and November, with 28.8% of the females having alpha atresia present. Spent females were characterized based on presence of POFs and a high percentage (>50%) of remaining advanced oocytes in an alpha atretic state. Most spent females were observed during the fall (Figure 6), towards the end of the spawning season, and they composed 11–12% of the fish in October and November. Two females in May were classified as spent (0.8% of May fish), having already completed spawning for the year (mean GSI = 3.21). This was also the case for the four resting females observed in April and May (1.5% and 1.2% of fish in those months, respectively; mean GSI = 0.36 for resting females in both months combined).

Immature females were more readily distinguished in spring when no mature females were observed with primary growth as the MAOS, and only two immature fish had early cortical alveolar oocytes as the MAOS in spring. In fall, both primary growth and cortical alveoli were observed in immature and resting females. The composition of the tunica was an important character for distinguishing these classes, and the presence of POFs often further distinguished most resting females.

More of the female Cusk classed as immature based on histology came from the later 6 months of the year ($n = 49$) than in the first half of the year ($n = 18$). The smallest mature female was 35 cm, and the largest immature female was 52 cm. The low number of immature fish from the spring surveys limited the ability to fit a seasonally specific model for size at maturity. However, the protracted spawning season of female Cusk and continued presence of spawning markers allowed the identification of mature spawning participants throughout the year. Therefore, histologically determined maturity from all months were used in determination of the final female maturity ogive. The final ogive model (Figure 7; slope = 0.454 [SE = 0.051], intercept = −17.910 [SE = 2.147], $n = 817$, residual deviance = 201.540) for female Cusk had a length at 50% maturity (L_{50}) = 39.468 cm (95% CI = 38.718–39.947).

Fecundity

Gravimetric fecundity estimates were obtained for 142 female Cusk prior to spawning. The autodiametric relationship was $NG = (9.250 \times 10^{10}) \times (OD^{-2.545})$, with a deviance explained of 0.930 (SE $a = 2.810 \times 10^{10}$, SE $b = 0.048$; OD range = 399–759 μm). Cusk PAF was estimated for females from 38 to 82 cm TL (Figure 8). The fecundity–length model including OD_{LC} had a lower AIC_c ($\Delta AIC_c = 4.255$; weight = 0.894) than the base model with only length. The resulting full model, $\ln(PAF) = (3.791 \times TL) + [(-7.940 \times 10^{-4}) \times OD_{LC}] - 0.760$, had an $r^2 = 0.824$ ($n = 142$; RSE = 0.289; SE $\beta_1 = 0.147$, SE $= 3.143 \times 10^{-4}$,

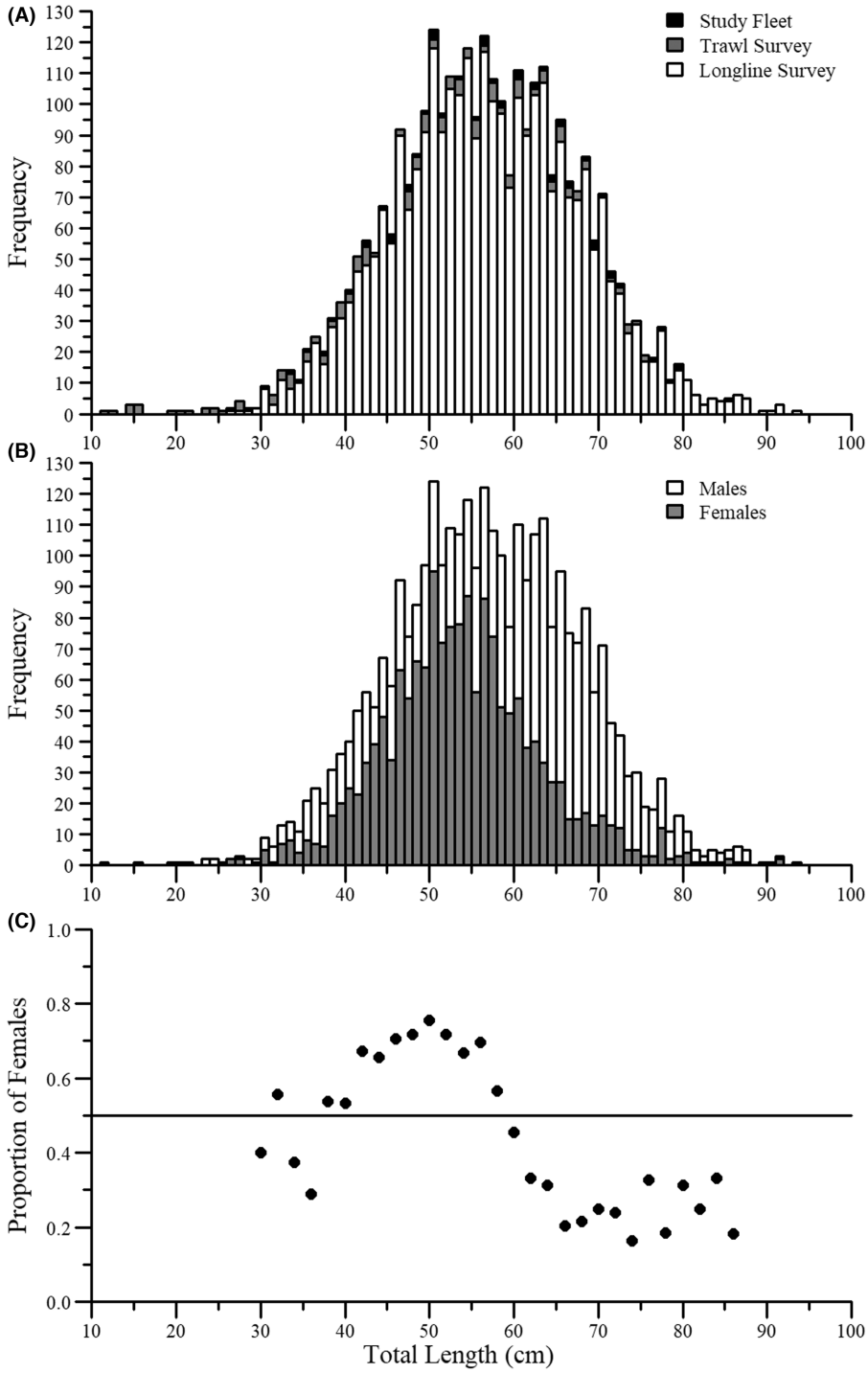

FIGURE 4. **(A)** Stacked length frequency distributions in 1-cm bins for all Cusk ($n = 3{,}188$) that were captured using different fishing gear types from the bottom trawl survey ($n = 166$), the bottom longline survey ($n = 2{,}972$), and the Study Fleet commercial samples, which were predominantly using rod-and-reel gear with a few fish from bottom trawls ($n = 50$). Panel **(B)** shows the length frequency distributions by sex for fish where it was available ($n = 3{,}172$), and panel **(C)** shows the proportion of females at each 2-cm increment shown for all length bins with greater than five individuals.

SE = 0.618). The slope of the length coefficient had significant positive allometry ($\beta_1 > 3.170$) relative to total length ($t = 4.209$, $P < 0.001$). The fecundity model estimates and length ranges in the current study were similar to those reported for Cusk on the Scotian Shelf in the 1960s (Figure 8; Oldham 1972).

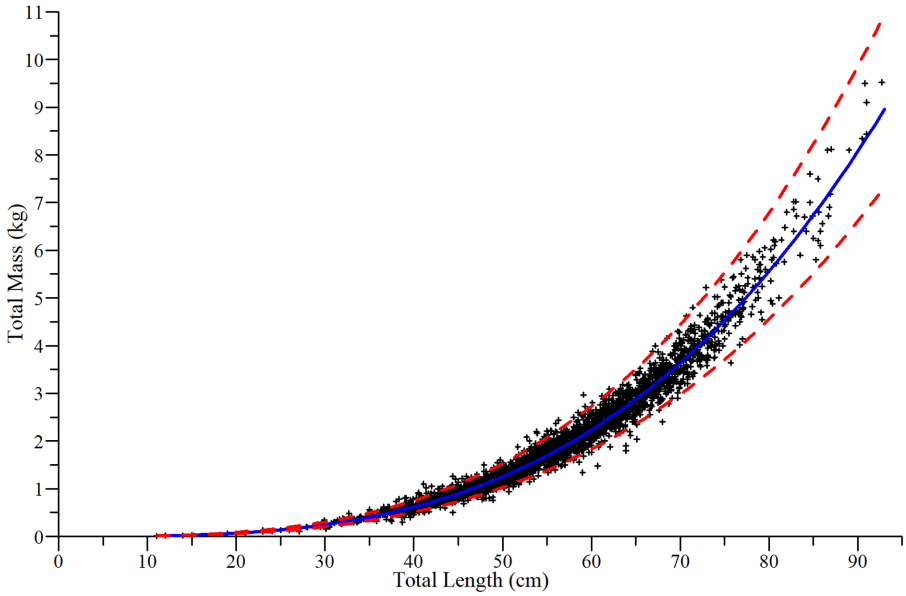

FIGURE 5. Plot of all total length and total mass data for sampled Cusk during 2013–2018 ($n = 3{,}160$). The solid blue line is the predicted model, and the dashed red lines indicate the 95% confidence region for the predicted model.

Male Reproductive Seasonality

Males had generally low GSI values (rarely >1.0) throughout the year, and the testes had spermatozoa present in all months examined. Measured spawning activity inferred from elevated GSI was greater in the spring but was also evident in later months (Figure 9). The majority (>60%) of males sampled each month from January to July had spermatozoa as the dominant stage in the testes, whereas in the fall, spermatogonia were the dominant stage in more than half of the samples (October and November). The GSI in males increased from April to June relative to other months, with the median being above 0.3 (Figure 9) and the lower quartiles being higher than the upper quartile of most other months. The observed range of male GSI in April and May was broader and more males exceeded 0.5 than in other months.

Spermatozoa were present in all male Cusk examined, including the smallest males sampled (21 cm TL; 10 fish <30 cm), some of which were examined in detail in the laboratory to obtain macroscopic images to accompany histology (Figure 3). The testes on these small males were thin, poorly vascularized, and translucent. Spermatozoa were present but composed less of a proportion of the testes than in the larger males. The SMI analysis supported this, with most of the smallest males (25–35 cm) having an index <0.3, and the majority of the fish with an index >0.4 were >40 cm TL (92%, $n = 71$; Figure 10). The majority of males (eight out of nine fish) with the lowest SMI values (SMI ≤0.3) were <37 cm, but there was some overlap of males with high and low SMI, particularly from ~33 to 40 cm TL. The limited testicular development when coupled with low GSI raises questions about whether these smaller males are "functionally" mature. However, the SMI still did not provide a clear differentiation in testes structural development across the length range examined. Due to the low numbers of clearly immature males based on histological criteria, a maturity ogive was not generated for males.

Hepatosomatic and Relative Condition

The hepatosomatic condition of Cusk was variable within months, with seasonal changes evident for both sexes. The median and quartiles of HSI were lower from April to June during the peak of spawning activity for both sexes, with the upper quartiles <4 and medians ~3 (Figure 11). The sample sizes were low, but the few winter-sampled fish were the highest (>5 HSI), and fish in the fall had interquartile ranges in HSI that were typically 3 to 5. The median and interquartile range of HSI within nearly all months was higher for females than males, with June being the exception.

Relative condition (gonad-free K_n) was also variable, and the interquartile range overlapped with 1.0 in all months that had a sample size greater than five (Figure 11). The median K_n for both sexes was at or below 1.0 (average condition) in April through June during this peak spawning period, with the lowest of the year for both being in June (female median $K_n = 0.949$–0.961; male median $K_n = 1.002$–1.016). Relative condition was low for

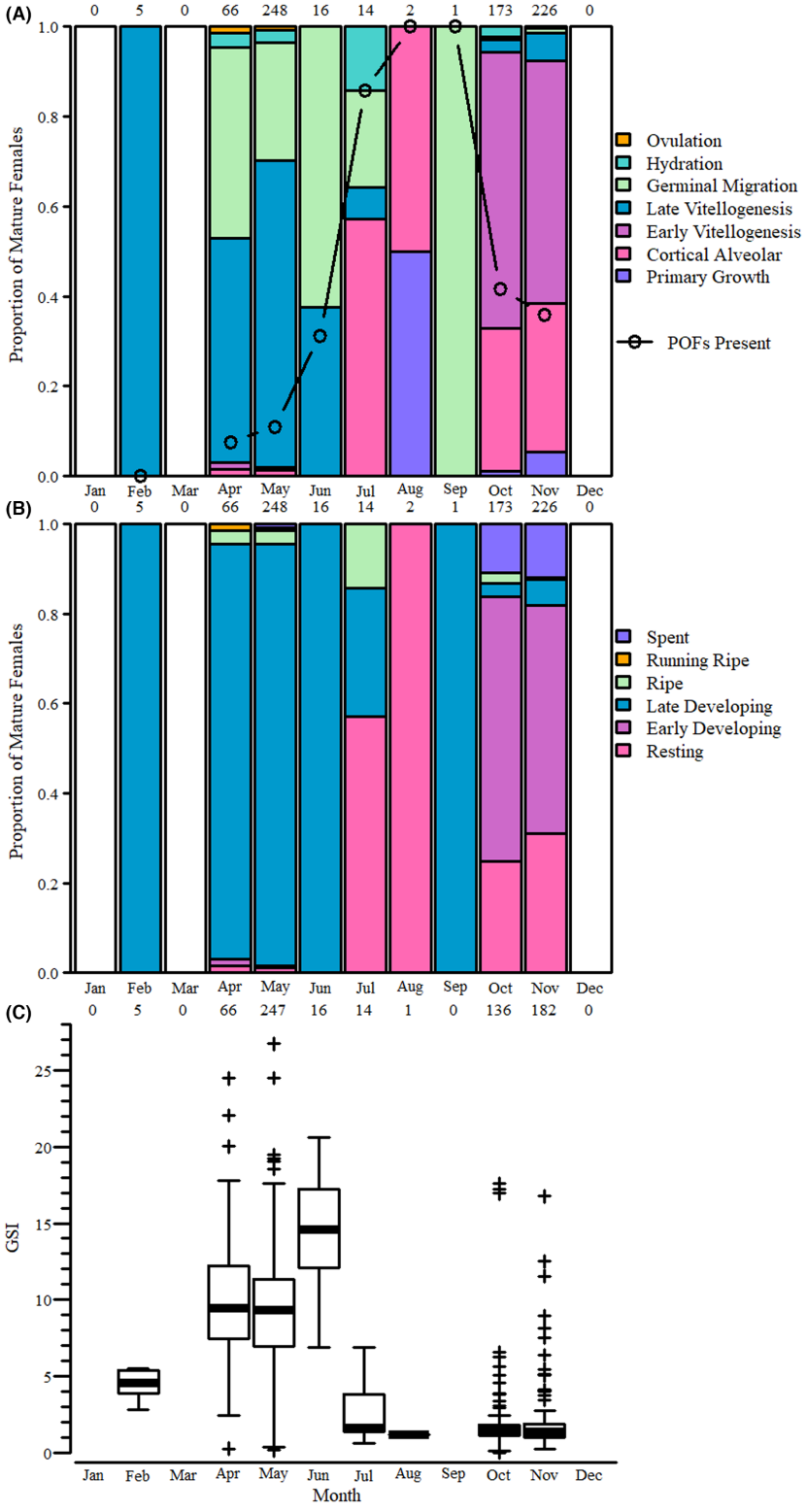

FIGURE 6. Seasonal pattern for mature female Cusk **(A)** in the most advanced oocyte stage, **(B)** by maturity class, and **(C)** based on the gonadosomatic index (GSI). Sample sizes are displayed above each month. In panel (A), the overlaid points and line indicate the proportion of females with postovulatory follicles (POFs) present. The germinal vesicle breakdown stage ($n = 1$) is included with hydration. For the box plots in panel (C), the horizontal line in each box indicates the median, the box dimensions represent the 25th–75th percentile ranges, the whiskers show 1.5× the interquartile range, and the plus signs indicate outliers.

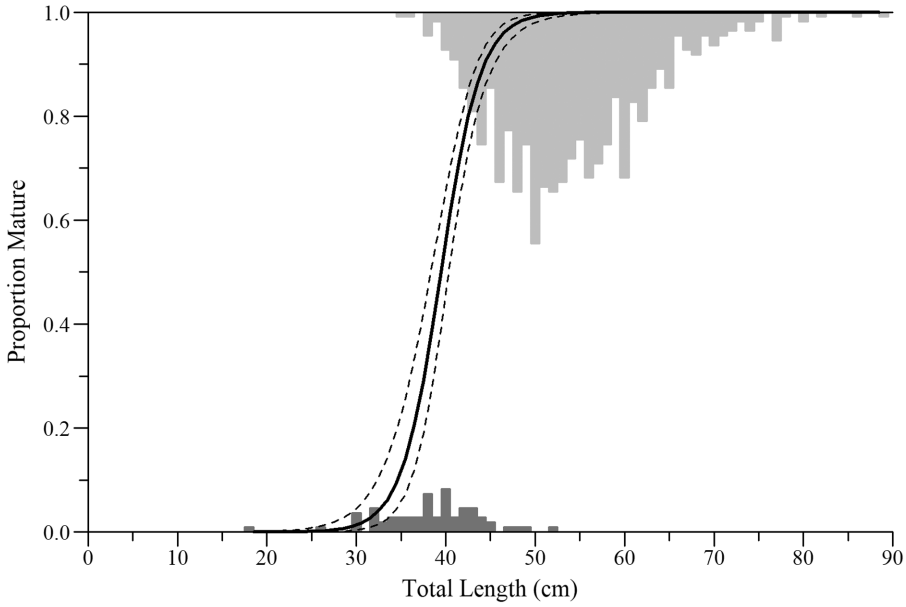

FIGURE 7. Model prediction (solid line) and 95% confidence interval (dashed lines) for proportion mature at length (1 = mature and 0 = immature) for female Cusk determined using ovarian histology. The length at 50% maturity (L_{50}) is 39.47 cm ($n = 817$). Also shown are the frequency distributions in 1-cm bins for immature (dark gray; $n = 67$) and mature females (light gray; $n = 750$).

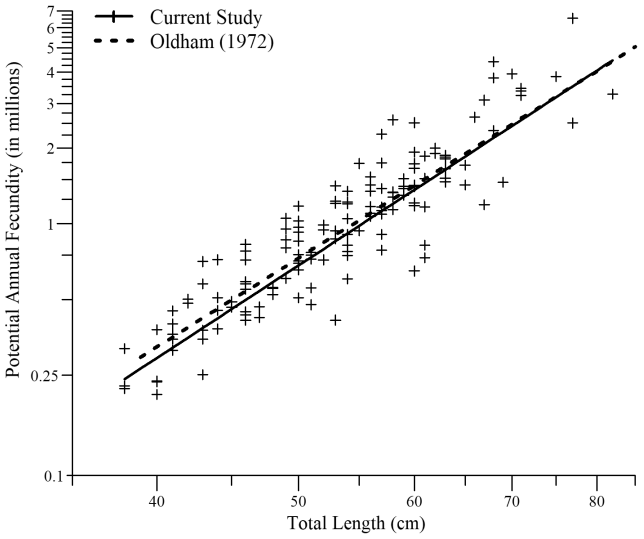

FIGURE 8. Potential annual fecundity (PAF) for Cusk plotted at length with both total length and PAF on a natural log scale. The solid line indicates predicted PAF at length for Cusk from the current study with a model including oocyte diameter of the leading cohort (prediction estimates made using $OD_{LC} = 800\,\mu m$). Predicted fecundity at length (dashed line) based on the model reported by Oldham (1972) is shown for the length range sampled in that study.

males in February, but only six samples were obtained. Males had a less variable K_n than females, and monthly medians were always above 1.0 (Figure 11). November had the highest median of all months with a sample size greater than 10 fish (female median $K_n = 1.000$; male median $K_n = 1.039$), and the limited samples during winter suggested that condition was higher then.

Age and Growth

Overall Cusk age estimates were precise as within-reader agreement achieved 71%. The average within-reader CV was 3%, and there was no systematic bias between original age and test ages (test of symmetry: $\chi^2 = 9.33$, df = 7, $P = 0.23$). Comparisons between the von Bertalanffy curves demonstrated that the null model, which assumed common growth coefficients for females and males, was significantly different ($\chi^2 = 1{,}705$, df = 3, $P = 0.0001$) than models with separate parameters by sex (Figure 12). Therefore, growth parameters for both males and females were estimated separately, with parameters for males of $L_\infty = 85.79$ cm, $k = 0.15$, and $t_0 = 0.37$ and for females of $L_\infty = 112.54$ cm, $k = 0.05$, and $t_0 = -3.73$.

DISCUSSION

The results of the current study provide the most complete biological data available for Cusk in the western North Atlantic. This study is the first to utilize gonad histology to evaluate maturity and spawning seasonality for Cusk. To be useful for management, life history parameters need to be from the appropriate region, accurate, and current. Therefore, the results herein are valuable to management and the stock assessment for this data-poor

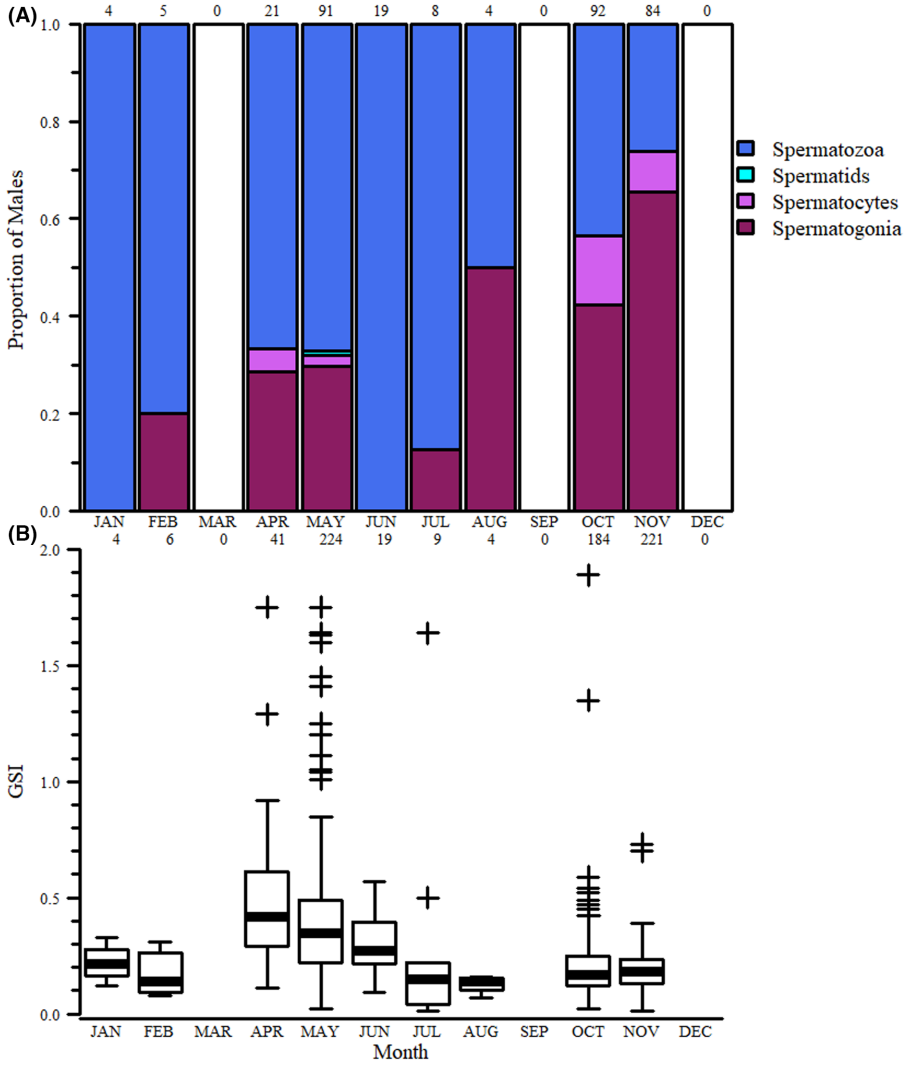

FIGURE 9. Seasonal pattern in male Cusk based on the **(A)** dominant stage of spermatogenesis and **(B)** gonadosomatic index (GSI). Sample sizes are displayed above each month. See Figure 6 for a definition of box plot elements.

species with an uncertain population status in U.S. waters (Tallack 2012).

Reproductive Seasonality

Cusk in the Gulf of Maine have a protracted spawning season that peaks in spring and extends into summer. Although seasonal coverage was variable, a high occurrence of spawning activity was identified in the spring (particularly May) and some sporadic spawning fish were identified throughout the summer and even into early fall. The spawning seasonality we observed is similar to earlier studies in the region and elsewhere. Bigelow and Schroeder (1953) reported Cusk in the Gulf of Maine spawning in spring and early summer, commonly into July. Cusk eggs in the Gulf of Maine and Georges Bank were collected from March until November, with peak egg abundance in May and June (Berrien and Sibunka 1999).

On the Scotian Shelf, spawning timing may be similar or with a slightly later onset and peak. Oldham (1972) reported spawning from May until August, with a peak in late June, and spawning was distributed over the whole region with no distinct spawning aggregations. Ichthyoplankton surveys from 1976 to 1982 (reported in Harris et al. 2002) captured Cusk eggs at Scotian Shelf stations May through September, with the highest occurrence May to July. European studies report similar April to June spawning, including off Iceland, Ireland, the Faroe Islands, and the Norwegian shelf (Magnússon et al. 1997).

Female Maturity

We present the first assessment of maturity for this species using ovarian histology, which has the benefit to improve the accuracy of maturity classification. Because the samples were predominantly captured via longline

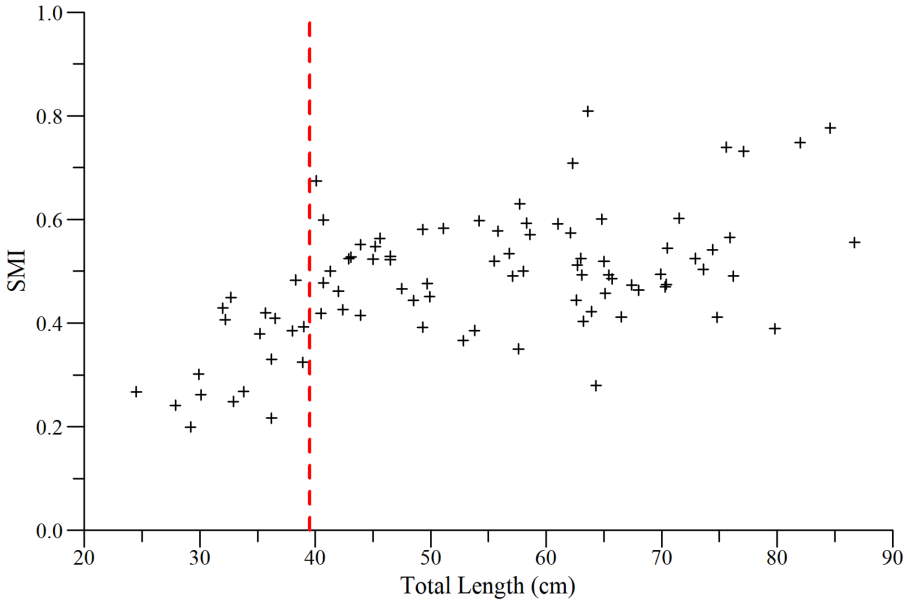

FIGURE 10. The spermatogenic maturity index (SMI) of male Cusk in relation to Cusk total length sampled in April and May ($n = 90$). For comparison, the L_{50} determined in the current study for female Cusk is shown (dashed red line).

with hook size targeting larger individuals, gear selectivity may have biased the collection of immature fish (e.g., only catching larger immature individuals). Combining samples from multiple gear types (e.g., trawl survey samples) helped to reduce this potential bias and improved the size distribution sampled. However, future work should focus on evaluation of smaller Cusk to improve the precision of the size at first maturity.

The female size at maturity found here is consistent with previous reports in the region based on macroscopic data (e.g., 37 cm for females and 44 cm for males; Tallack 2012). Earlier more comprehensive maturity work in the 1960s on the Scotian Shelf that included eastern portions of the Gulf of Maine (Oldham 1972) found a larger L_{50} for females of 50.7 cm (aged 6.5 years) than the current study. Later work on the Scotian Shelf by Beacham (1982) found a lower size at maturity for females in the more eastern Northwest Atlantic Fisheries Organization subdivision 4X region ($L_{50} = 47$ cm) than the 4W region (56 cm). The size at maturity from macroscopic survey data from the 1950s–1970s did not differ significantly among decades when sample sizes were sufficient to compare (Beacham 1982). More recent analyses of macroscopic data reported an L_{50} for Canadian Fisheries and Oceans Canada data of 42 cm and 39 cm for the U.S. NEFSC data (COSEWIC 2012). These estimates based on macroscopic determinations are similar to the present study using ovarian histology. The differences in size at maturity between the earliest available data and more contemporary reports could be related to geographic or methodological differences as well as temporal changes. Differences in observed maturity over time and among regions could be influenced by changes in the population size, environmental factors, intrinsic population differences, fishing mortality rates, or other abiotic or biotic factors (Olsen et al. 2005; Nash et al. 2010; Miller et al. 2018). Future work should focus on collecting and characterizing the maturity and age data across the Gulf of Maine and Scotian Shelf to evaluate regional and temporal variation across both U.S. and Canadian waters.

Reports from the eastern Atlantic Ocean on Cusk maturity are also limited but indicate similar size at maturity as found in the western Atlantic Cusk. From combined sampling efforts by Norway, Iceland, and the Faroe Islands, Magnússon et al. (1997) reported Cusk mature at 8–10 years (40–45 cm). Bergstad and Hareide (1996) reported an age at 50% maturity (A_{50}) of 6–7 years for females, and although they did not report an L_{50}, based on their reported size at age, this would have been approximately 35–45 cm depending on the region. They sampled from commercial long-liners throughout the year and indicated that macroscopic determination of the immature and resting/recovering classes of fish was challenging at certain times of the year. These limited estimates of size at maturity come from disparate fishing locations, and finer-scale sampling is required to evaluate variation in maturity within both the eastern and western Atlantic Ocean populations.

Fecundity

The best fecundity model developed in the present study included OD of the leading cohort, similar to

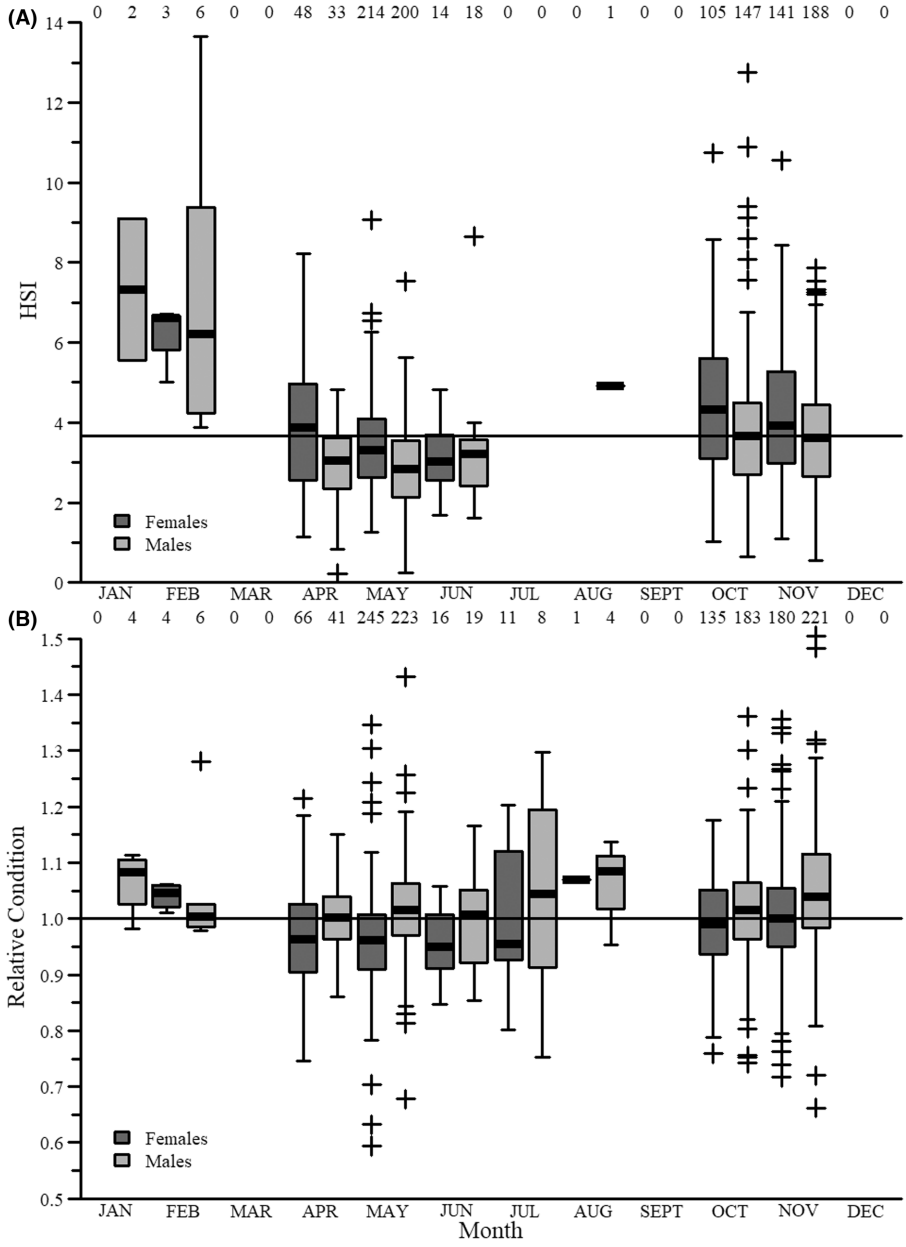

FIGURE 11. The **(A)** hepatosomatic index (HSI) and **(B)** relative condition of female and male Cusk by month sampled. Female data are for only mature fish, whereas male data include all fish sampled. Relative condition (K_n) was calculated using length–mass relationships determined for gonad-free fish mass. Reference lines of "average" condition ($K_n = 1.0$) and the calculated average HSI (3.66) are shown. Sample sizes are shown above each month. See Figure 6 for a definition of box plot elements.

fecundity studies on other species that show a general decline in PAF as OD_{LC} increases (McElroy et al. 2016). The OD serves as a proxy for the individual level of clutch development, and including it should partially account for the down-regulation (as indicated by the negative slope of the OD_{LC} term) on the estimates of PAF. The inclusion of OD_{LC} in the model results in estimates of potential fecundity being closer to realized fecundity. The use of ovarian histology to identify fish that had started spawning and OD_{LC} from oocyte size frequencies to account for down-regulation both improved the accuracy of the PAF estimates. The autodiametric relationship reported here enables more efficient estimation of fecundity for exploring spatial and temporal patterns in fecundity over larger scales.

The fecundity-at-length relationship reported here is remarkably similar to the only previous data in the western Atlantic Ocean by Oldham (1972), which was

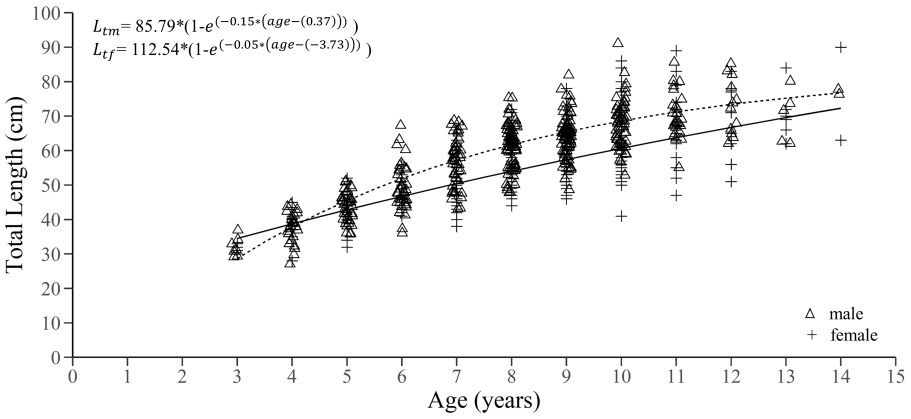

FIGURE 12. Observed length at age and fitted von Bertalanffy model for Cusk collected in the Gulf of Maine from 2016 to 2017 ($n = 1{,}041$). The fitted model is presented for total length at time t (L_t) for females (f) and males (m), shown by the solid and dashed line, respectively.

conducted on the Scotian Shelf. The results were similar despite 50 years and the previous work not having the benefit of ovarian histology to omit any fish that had commenced spawning. Cusk fecundity ranged from a quarter million to over four million eggs, which was also comparable to other large gadoids with group-synchronous oocyte development in the region. Fecundity of Atlantic Cod on Georges Bank ranges from a few hundred thousand to over five million eggs, and Haddock on Georges Bank and the Grand Banks can have a fecundity from 100,000 to just under three million eggs but achieve a smaller maximal size than Atlantic Cod (Almeida et al. 2009; Rogers et al. 2019).

The fecundity of Cusk has positive allometric increases, which were greater than just proportional to increasing fish size. This relationship of fecundity relative to fish size should be taken into consideration when examining the reproductive potential for a species. It emphasizes the importance of the largest females to the reproductive output of a population (Hixon et al. 2014; Barneche et al. 2018), although the scale of the impact on population reproductive output may only be ~10% when taking into account population demographics (Andersen et al. 2019). The scaling of the fecundity and body size relationship has been found to vary, but nonisometric scaling with body size has been reported in a variety of fish taxa (Stafford et al. 2014; Barneche et al. 2018; Lefebvre et al. 2019). Fecundity scaling does not account for other reproductive attributes of large(r) females such as egg size or energy content, which can also have benefits for larval size and survival (Berkeley et al. 2004; Trippel and Neil 2004; Hixon et al. 2014). The increased relative fecundity for larger females indicates that both spawning stock biomass and stock demographics ultimately determine stock reproductive potential.

Male Maturity

In contrast to females, male Cusk appear to have lower reproductive investment (as indicated by GSI) compared with other gadids in the region. The GSI of male Cusk during the spawning season was always below 2, whereas male Atlantic Cod GSI is typically >2 and can be as high as 15 (Trippel and Morgan 1994). It is unlikely that we missed actively spawning males having a higher GSI entirely due to some gear or behavioral selectivity, for the following reasons. First, we sampled with multiple gears (having different selectivity) and caught many male fish in the same months (and locations) as developing and spawning females. While spawning males may not have been feeding, and thus missed, this would result in an increase in percentage females at size (during spawning months), which is the opposite of what we observed. Second, if prespawning males are not feeding (i.e., taking hooks), it seems highly unlikely that, given our large sample size, we would not have collected some fish at least beginning to ramp up their GSI. The GSI of Atlantic Cod is elevated for several months prior to spawning (Almeida et al. 2009); therefore, we feel it is unlikely (1) that male Cusk do not feed for many months of the year and (2) that we would not have caught at least some that were ramping up. If mature males do not feed for many months of the year, we would expect their growth to be slower, which is not supported by the size at age data presented, and assuming we collected postspawning fish, their relative condition would be reduced following spawning, which was also not evident. Third, we find it unlikely that so many males would be nonparticipatory (i.e., excluded from actively spawning by cryptic male spawners) given that males of most species (including gadids) mature at earlier ages and smaller sizes than females do, and we collected many large males up to the largest sizes sampled during the spawning season. Low GSI of male fish is

sometimes associated with low fecundity, nest guarding, or internal fertilization, but Cusk have pelagic eggs and no secondary structures associated with internal fertilization. Males defending females or spawning sites often have low levels of sperm production compared with high sperm production in species with higher sperm competition (Petersen and Mazzoldi 2010). High fertilization rates (and low GSI) have been associated with species that spawn in pairs and in nests or confined habitats that may retain sperm for long periods (Petersen and Mazzoldi 2010). Cusk have been observed (e.g., via remotely operated vehicle) to inhabit complex rocky structures, such as boulders and ledges, or to find refuge among corals and sponges (Auster and Lindholm 2005; Kutti et al. 2015; Ross et al. 2015). In addition, given the low temperatures preferred by Cusk, sperm are likely viable for over an hour as for Atlantic Cod (Trippel and Morgan 1994). Although the eggs of Cusk are pelagic, it is possible that spawning or mating or fertilization occurs in a manner (pairs) and confined "nests" that permit high fertilization rates with low sperm production. The mating behaviors of Cusk are unknown but warrant investigation to understand why males have such low GSI.

Regardless of the reasons for low GSI in males, this has implications with respect to energy allocation. The lower reproductive investment by males could make more energy available for growth or spawning behavior (guarding females or breeding site) or enable spawning over a more protracted spawning season. Significant migration and movement has been suggested as unlikely for Cusk in multiple regions (Bigelow and Schroeder 1953; Johansen and Nævdal 1995; Knutsen et al. 2009); however, their seasonal movements are not well known, without any known tagging studies on the species to date. The low GSI of males and limited seasonal change in gonad size and appearance complicate macroscopic classification. The histological analysis of males was also equivocal due to the presence of advanced sperm stages in even the smallest males examined. Despite the presence of advanced sperm in these small males, the small size of the gonad and lower percentage of area with advanced sperm make it unlikely that these individuals are functionally mature. The SMI calculations provided a means to quantify this, and although the results are somewhat ambiguous, there is an increase in SMI for males around 35–40 cm, corresponding to the size at onset of maturity in females. Oldham (1972) reported male maturity at 43.5 cm and 4.7 years based on macroscopic criteria. We found that traditional macroscopic and microscopic methods failed to provide definitive diagnosis of the onset of maturity in males, but the data suggest the vast majority of males collected were mature.

The sex-specific differences in growth are likely the result of this differential reproductive investment, with males expending less energy towards reproduction and more to growth. Both sexes showed similar seasonal patterns in HSI and relative condition, and scale of HSI was relatively similar between the sexes and comparable to that of other gadids in the region (Atlantic Cod HSI = 1.86–9.96, Haddock HSI = 1.56–8.46; Alonso-Fernandez et al. 2009). Female Cusk had slightly higher HSI, which may be related to the energetic requirements of vitellogenin production. The gonad-free K_n of male Cusk was consistently higher than that of females and did not show as dramatic a decline during or after spawning in spring. The more stable K_n of males throughout spawning and the entire year may be indicative of the limited energetic investment to reproduction compared with females.

Sex Ratio

The change in sex ratio at increasing lengths may be influenced by several factors, including sex-specific selectivity of the surveyed habitat and fishing gear (where larger males are captured more efficiently), sex-specific differences in mortality (where females have lower survival), or sex-specific differences in growth (where males grow faster and achieve larger size at age than females). The latter is the most parsimonious explanation and is supported by our observations on reproductive investment, condition, and size at age. Oldham (1972) also reported higher proportions of males among the larger sizes of Cusk on the Scotian Shelf. Interestingly, Bergstad and Hareide (1996) did not find strong differences in growth between the sexes in the eastern Atlantic Ocean. Larger male size may be advantageous (i.e., selected for) if they guard females or sites during spawning (as in many protogynous hermaphrodites). More information on gear selectivity, spawning behaviors, and mortality of this enigmatic species would help to affirm these results on size composition.

Growth

Cusk otoliths are difficult to interpret. Baking the whole otolith did increase the contrast between the annuli, which in turn increased interpretation and precision. Overall, our precision of 70% for this species is much higher than the 30% to 40% achieved previously (Bergstad and Hareide 1996; Bergstad et al. 1998). Our differences in age estimates were mostly within 1 year (88% agreement ±1 year). Unlike Bergstad and Hareide (1996) and Magnussen (2007), our data showed there was a clear difference of mean age at length between sexes, with males growing larger at age. When estimating growth using the von Bertalanffy model, model fits were poor and had difficulty converging and the female growth curve ended up closer to linear than asymptotic, probably due to the lack of younger ages. Overall, our mean length at age was larger than other studies conducted in the eastern Atlantic Ocean (Bergstad and Hareide 1996; Jennings et al. 1999; Magnussen 2007). However, changes in the processing of

otoliths to increase precision of age estimates elsewhere could help confirm the differences in growth between sexes and across regions presented here.

Management Implications

Cusk are a managed species in U.S. waters but currently lack a formal stock assessment due to deficiencies in long-term data and remain a NOAA species of concern. There are currently no size or quota limits on this species. Contemporary data on the maturity, sexual dimorphism, age and growth, and spawning seasonality are valuable to the development of sustainable management for this species. These data will inform managers if they look to establish minimum sizes and other regulations in the future. The life history, limited movements, and preference for rocky habitat and cold water by Cusk make it of increased vulnerability to climate change (Hare et al. 2012, 2016). Cusk are considered to have a high biological sensitivity and climate exposure, and their overall climate vulnerability in U.S. waters is expected to be in a negative direction (Hare et al. 2016). Obtaining current data on the life history is necessary for monitoring how these parameters may respond to a changing environment. The data presented here fill substantial gaps in our understanding of Cusk biology and advance the information available for status assessments of this data-poor species in U.S. waters.

ACKNOWLEDGMENTS

We thank Captains P. Lynch (FV *Mary Elizabeth)* and E. Hesse (FV *Tenacious II*) and their crews for contributions to the bottom longline survey and collection of these samples. We thank the Cooperative Research Branch staff for their support collecting samples during the BLLS, in particular C. Alexander, B. Gervelis, G. Gianesin, and D. St. Amand. We are grateful to staff of the Ecosystems Surveys Branch for their efforts on the bottom trawl survey and the work of the captain and crews of the NOAA ship *Henry B. Bigelow*. We appreciate the contributions of the collaborating industry vessels of the Cooperative Research Branch Study Fleet. We are grateful for the work of S. Emery for aging the Cusk samples. Special thanks to L. O'Brien for contributions to the design of the BLLS and many discussions about the life history of Cusk. We appreciate the comments of M. Terceiro, A. Mercer, and two anonymous reviewers on earlier versions of this manuscript. Mention of any products is for descriptive purposes and does not indicate endorsement by NOAA Fisheries. There is no conflict of interest declared in this article.

ORCID

Mark J. Wuenschel https://orcid.org/0000-0002-9307-7319

REFERENCES

Almeida, F. F. L., G. L. Taranger, B. Norberg, Ø. Karlsen, J. Bogerd, and R. W. Schulz. 2009. Photoperiod-modulated testis maturation in Atlantic Cod (*Gadus morhua*, L.). Biology of Reproduction 80:631–640.

Alonso-Fernandez, A., A. C. Vallejo, F. Saborido-Rey, H. Murua, and E. A. Trippel. 2009. Fecundity estimation of Atlantic Cod (*Gadus morhua*) and Haddock (*Melanogrammus aeglefinus*) of Georges Bank: application of the autodiametric method. Fisheries Research 99:47–54.

Andersen, K. H., N. S. Jacobsen, and P. D. van Denderen. 2019. Limited impact of big fish mothers for population replenishment. Canadian Journal of Fisheries and Aquatic Sciences 76:347–349.

Anderson, D. R. 2008. Model based inference in the life sciences: a primer on evidence. Springer Science & Business Media, New York.

Auster, P. J., and J. Lindholm. 2005. The ecology of fishes on deep boulder reefs in the western Gulf of Maine (NW Atlantic). Pages 89–107 *in* J. M. Godfrey and S. E. Shumway, editors. Diving for science 2005: proceedings of the American Academy of Underwater Science 24th annual symposium. American Academy of Underwater Sciences, Dauphin Island, Alabama.

Barneche, D. R., D. R. Robertson, C. R. White, and D. J. Marshall. 2018. Fish reproductive-energy output increases disproportionately with body size. Science 360:642–644.

Beacham, T. D. 1982. Median length at sexual maturity of Halibut, Cusk, Longhorn Sculpin, Ocean Pout, and Sea Raven in the Maritimes area of the northwest Atlantic. Canadian Journal of Zoology 60:1326–1330.

Bergstad, O. A., and N.-R. Hareide, editors. 1996. Ling, Blue Ling and tusk of the north-east Atlantic. Havforskningsinstituttet, Bergen, Norway.

Bergstad, O. A., J. V. Magnússon, J. Magnússon, N.-R. Hareide, and J. Reinert. 1998. Intercalibration of age readings of Ling (*Molva molva* L.), Blue Ling (*Molva dipterygia* Pennant, 1784) and tusk (*Brosme brosme* L.). International Council for the Exploration of the Sea Journal of Marine Science 55:309–318.

Berkeley, S. A., C. Chapman, and S. M. Sogard. 2004. Maternal age as a determinant of larval growth and survival in a marine fish, *Sebastes melanops*. Ecology 85:1258–1264.

Berrien, P., and J. Sibunka. 1999. Distribution patterns of fish eggs in the U.S. northeast continental shelf ecosystem, 1977–1987. NOAA Technical Report NMFS 145.

Bigelow, H. B., and W. C. Schroeder. 1953. Fishes of the Gulf of Maine. U.S. Fish and Wildlife Service Fishery Bulletin 53.

Bowker, A. H. 1948. A test for symmetry in contingency tables. Journal of the American Statistical Association 43:572–574.

Campana, S. E., and C. M. Jones. 1992. Analysis of otolith microstructure data. Canadian Special Publication of Fisheries and Aquatic Sciences 117:73–100.

Cohen, D. M., T. Inada, T. Iwamoto, and N. Scialabba. 1990. Gadiform fishes of the world (order Gadiformes). An annotated and illustrated catalogue of cods, hakes, grenadiers and other gadiform fishes known to date. FAO species catalogue, volume 10. (Food and Agriculture Organization) Fisheries Synopsis 125.

COSEWIC (Committee on the Status of Endangered Wildlife in Canada). 2012. COSEWIC assessment and status report on the Cusk *Brosme brosme* in Canada. COSEWIC, Ottawa.

Davies, T. D., and I. D. Jonsen. 2011. Identifying nonproportionality of fishery-independent survey data to estimate population trends and assess recovery potential for Cusk (*Brosme brosme*). Canadian Journal of Fisheries and Aquatic Sciences 68:413–425.

DFO (Fisheries and Oceans Canada). 2019. Stock status update of Cusk (*Brosme brosme*) in NAFO Divisions 4VWX5YZ. Canadian Science Advisory Secretariat Science Responses 2019/013.

Fahay, M. P. 2007. Early stages of fishes in the western North Atlantic Ocean. (Davis Strait, Southern Greenland and Flemish Cap to Cape Hatteras), volumes 1 and 2. Northwest Atlantic Fisheries Organization, Dartmouth, Nova Scotia.

Hare, J. A., J. P. Manderson, J. A. Nye, M. A. Alexander, P. J. Auster, D. L. Borggaard, A. M. Capotondi, K. B. Damon-Randall, E. Heupel, I. Mateo, L. O'Brien, D. E. Richardson, C. A. Stock, and S. T. Biegel. 2012. Cusk (*Brosme brosme*) and climate change: assessing the threat to a candidate marine fish species under the U.S. Endangered Species Act. ICES (International Council for the Exploration of the Sea) Journal of Marine Science 69:1753–1768.

Hare, J. A., W. E. Morrison, M. W. Nelson, M. M. Stachura, E. J. Teeters, R. B. Griffis, M. A. Alexander, J. D. Scott, L. Alade, R. J. Bell, A. S. Chute, K. L. Curti, T. H. Curtis, D. Kircheis, J. F. Kocik, S. M. Lucey, C. T. McCandless, L. M. Milke, D. E. Richardson, E. Robillard, H. J. Walsh, M. C. McManus, K. E. Marancik, and C. A. Griswold. 2016. A vulnerability assessment of fish and invertebrates to climate change on the northeast U.S. continental shelf. PLoS (Public Library of Science) ONE 11(2):e0146756.

Harris, L. E., P. A. Comeau, and D. S. Clark. 2002. Evaluation of Cusk (*Brosme brosme*) in Canadian Waters. Fisheries and Oceans Canada Canadian Science Advisory Secretariat Research Document 2002/104, Dartmouth.

Hixon, M. A., D. W. Johnson, and S. M. Sogard. 2014. BOFFFFs: on the importance of conserving old-growth age structure in fishery populations. ICES (International Council for the Exploration of the Sea) Journal of Marine Science 71:2171–2185.

Jennings, S., S. P. R. Greenstreet, and J. D. Reynolds. 1999. Structural change in an exploited fish community: a consequence of differential fishing effects on species with contrasting life histories. Journal of Animal Ecology 68:617–627.

Johansen, T., and G. Nævdal. 1995. Genetic analysis of population structure of tusk in the North Atlantic. Journal of Fish Biology 47: 226–242.

Jones, A. W., K. A. Burchard, A. M. Mercer, J. J. Hoey, M. D. Morin, G. L. Gianesin, J. A. Wilson, C. R. Alexander, B. A. Lowman, D. G. Duarte, D. Goethel, J. Ford, J. Ruhle, R. Sykes, and T. Sawyer. 2022. Learning from the Study Fleet: maintenance of a large-scale reference fleet for northeast U.S. fisheries. Frontiers in Marine Science 9:869560.

Kimura, D. K. 1980. Likelihood methods for the von Bertalanffy growth curve. U.S. National Marine Fisheries Service Fishery Bulletin 77:765–776.

Knutsen, H., P. E. Jorde, H. Sannæs, A. Rus Hoelzel, O. A. Bergstad, S. Stefanni, T. Johansen, and N. C. Stenseth. 2009. Bathymetric barriers promoting genetic structure in the deepwater demersal fish tusk (*Brosme brosme*). Molecular Ecology 18:3151–3162.

Kutti, T., J. H. Fossa, and O. A. Bergstad. 2015. Influence of structurally complex benthic habitats on fish distribution. Marine Ecology Progress Series 520:175–190.

Le Cren, E. D. 1951. The length-weight relationship and seasonal cycle in gonad weight and condition in the perch (*Perca fluviatilis*). Journal of Animal Ecology 20:201–219.

Lefebvre, L. S., C. L. Friedlander, and J. C. Field. 2019. Reproductive ecology and size-dependent fecundity in the Petrale Sole (*Eopsetta jordani*) in waters of California, Oregon, and Washington. U.S. National Marine Fisheries Service Fishery Bulletin 117:291–302.

Magnussen, E. 2007. Interpopulation comparison of growth patterns of 14 fish species on Faroe Bank: are all fishes on the bank fast-growing? Journal of Fish Biology 71:453–475.

Magnússon, J. V., O. A. Bergstad, N.-R. Hareide, J. Magnússon, and J. Reinert. 1997. Ling, Blue Ling, and Tusk of the northeast Atlantic. TemaNord 1997:535. Nordic Council of Ministers, Copenhagen.

McElroy W. D., L. O'Brien, J. Blaylock, M. H. Martin, P. J. Rago, J. J. Hoey, and V. A. Sheremet. 2019. Design, implementation, and results of a cooperative research Gulf of Maine longline survey, 2014–2017. NOAA Technical Memorandum NMFS-NE-249.

McElroy, W. D., M. J. Wuenschel, E. K. Towle, and R. S. McBride. 2016. Spatial and annual variation in fecundity and oocyte atresia of Yellowtail Flounder, *Limanda ferruginea*, in U.S. waters. Journal of Sea Research 107:76–89.

McMillan, D. B. 2007. Fish histology: female reproductive systems. Springer, Dordrecht, The Netherlands.

Miller, T. J., L. O'Brien, and P. S. Fratantoni. 2018. Temporal and environmental variation in growth and maturity and effects on management reference points of Georges Bank Atlantic Cod. Canadian Journal of Fisheries and Aquatic Sciences 75:2159–2171.

Murua, H., and F. Saborido-Rey. 2003. Female reproductive strategies of marine fish species of the North Atlantic. Journal of Northwest Atlantic Fishery Science 33:23–31.

Nash, R. D. M., G. M. Pilling, L. T. Kell, P.-J. Schön, and O. S. Kjesbu. 2010. Investment in maturity at age and length in northeast Atlantic Cod stocks. Fisheries Research 104:89–99.

Oldham, W. S. 1972. Biology of Scotian shelf Cusk, *Brosme brosme*. International Commission of the Northwest Atlantic Fisheries Research Bulletin 9:85–98.

Olsen, E. M., G. R. Lilly, M. Heino, M. J. Morgan, J. Brattey, and U. Dieckmann. 2005. Assessing changes in age and size at maturation in collapsing populations of Atlantic Cod (*Gadus morhua*). Canadian Journal of Fisheries and Aquatic Sciences 62:811–823.

Petersen, C. W., and C. Mazzoldi. 2010. Fertilization in marine fishes: a review of the data and its application to conservation biology. Pages 203–239 *in* K. S. Cole, editor. Reproduction and sexuality in marine fishes: patterns and processes. University of California Press, Oakland.

Politis, P. J., J. K. Galbraith, P. Kostovick, and R. W. Brown. 2014. Northeast Fisheries Science Center bottom trawl survey protocols for the NOAA ship Henry B. Bigelow. National Oceanic and Atmospheric Administration, Northeast Fisheries Science Center, Reference Document 14-06, Woods Hole, Massachusetts.

Ricker, W. E. 1975. Computation and interpretation of biological statistics of fish populations. Bulletin of the Fisheries Research Board of Canada 191.

Rogers, R., S. Rowe, R. M. Rideout, and M. J. Morgan. 2019. Fecundity of Haddock (*Melanogrammus aeglefinus*) off southern Newfoundland. Fisheries Research 220:105339.

Ross, S. W., M. Rhode, and A. M. Quattrini. 2015. Demersal fish distribution and habitat use within and near Baltimore and Norfolk Canyons, U.S. middle Atlantic slope. Deep Sea Research Part I: Oceanographic Research Papers 103:137–154.

Rountree, R. A., and F. Juanes. 2010. First attempt to use remotely operated vehicle to observe soniferous fish behavior in the Gulf of Maine, western Atlantic Ocean. Current Zoology 56:90–99.

Stafford, D. M., S. M. Sogard, and S. A. Berkeley. 2014. Maternal influence on timing of parturition, fecundity, and larval quality in three shelf rockfishes (*Sebastes* spp.). Aquatic Biology 21:11–24.

Tallack, S. 2012. Workshop on proactive conservation planning for northwest Atlantic Cusk. Gulf of Maine Research Institute, Portland, Maine.

Tholke, E. K., W. D. McElroy, and R. S. McBride. 2019. Spermatogenesis, reproductive maturation, and spawning seasonality of male Winter Flounder, *Pseudopleuronectes americanus*: comparisons among fishery stocks. Fisheries Research 214:85–97.

Tomkiewicz, J., T. M. N. Kofoed, and J. S. Pedersen. 2011. Assessment of testis development during induced spermatogenesis in the European Eel *Anguilla Anguilla*. Marine and Coastal Fisheries: Dynamics, Management, and Ecosystem Science 3:106–118.

Trippel, E. A., and M. J. Morgan. 1994. Age-specific paternal influences on reproductive success of Atlantic Cod (*Gadus morhua* L.) of the Grand Banks, Newfoundland. ICES (International Council for the Exploration of the Sea) Marine Science Symposia 198:414–422.

Trippel, E. A., and S. R. E. Neil. 2004. Maternal and seasonal differences in egg sizes and spawning activity of northwest Atlantic Haddock (*Melanogrammus aeglefinus*) in relation to body size and condition. Canadian Journal of Fisheries and Aquatic Sciences 61:2097–2110.

Wootton, R. J. 1990. Ecology of teleost fishes. Chapman and Hall, New York.